British Journal of Pharmacology (2001) 132, 1365–1373

www.nature.com/bjp

Chronic vascular toxicity of doxorubicin in an organ-cultured artery

[1]Takahisa Murata, [1]Hideyuki Yamawaki, [1]Masatoshi Hori, [1]Koichi Sato, *,[1]Hiroshi Ozaki & [1]Hideaki Karaki

[1]Department of Veterinary Pharmacology, Graduate School of Agriculture and Life Sciences, The University of Tokyo, Yayoi 1-1-1, Bunkyo-ku, Tokyo 113-8657, Japan

1 We investigated the chronic effects of doxorubicin (DXR) on morphological and functional changes in the rabbit mesenteric artery using an organ culture system.

2 In arteries cultured with 0.3 μM DXR for 7 days, the contractions induced by noradrenaline, but not those induced by endothelin-1 or high K^+, were strongly inhibited. This reaction was followed by a decrease in the induction of the α_{1A}-adrenoceptor without any change in the mRNA level. Inhibition of noradrenaline-induced contractions by DXR was attenuated by superoxide dismutase, and α_{1A}-adrenoceptor protein expression recovered.

3 In the arteries cultured with 1 μM DXR for 7 days, contractions induced by endothelin-1 or high K^+ and absolute force in the permeabilized muscles were also inhibited. Morphological examinations revealed the existence of concentrated nuclei and terminal deoxynucleotidyl transferase-mediated dUTP nick-end labelling (TUNEL)-positive smooth muscle cells, and internucleosomal DNA fragmentation was also detected, indicating the induction of apoptosis.

4 In the arteries cultured with 10 μM DXR for 7 days, nuclear swelling, karyolysis and random DNA fragmentation indicative of necrosis were observed, and muscle contractility was abolished.

5 These results suggest that 0.3 μM DXR selectively down-regulates the α_{1A}-adrenoceptor protein expression, resulting in a decrease in the noradrenaline-induced contraction. This down-regulation may be at least partly due to the production of a superoxide radical. DXR also caused a decrease in muscle contractility followed by apoptotic changes at 1 μM and necrotic changes at 10 μM. These changes might be responsible for the disturbance of the circulatory system that is often observed during the course of repetitive chemotherapy.

British Journal of Pharmacology (2001) **132,** 1365–1373

Keywords: Doxorubicin; rabbit mesenteric artery; apoptosis; α_{1A}-adrenoceptor; smooth muscle contractility

Abbreviations: DXR, doxorubicin; ET-1, endothelin-1; GAPDH, glyceraldehydes 3-phosphate dehydrogenase; NA, noradrenaline; SOD, superoxide dismutase; TUNEL, terminal deoxynucleotidyl transferase-mediated dUTP nick-end labelling

Introduction

Doxorubicin (DXR) is one of the most widely used broad-spectrum anticancer agents (Weiss *et al*., 1986). However, because this agent produces a chronic and dose-related cardiomyopathy as its principal side effect (Von Hoff *et al*., 1979; Young *et al*., 1981), its clinical utility is limited.

DXR can intercalate with DNA and change DNA functions, such as inhibition of DNA and RNA synthesis (Chuang & Chuang 1979), causing strand breaks to occur and inducing of apoptosis (Muller *et al*., 1997). These cytotoxicities are believed to be mediated either by an inhibition of DNA topoisomerase II (Chuang & Chuang 1979; Kusumoto *et al*., 1996) or by the generation of free radicals (Muller *et al*., 1997). The production of superoxide radical anions by oxidation-reduction cycling of DXR is of critical importance in mediating the chronic cardiotoxicity associated with the clinical use of DXR (Jeyaseelan *et al*., 1997).

Imbalances of the circulatory system such as decreases in blood pressure are often observed in clinical situations during repetitive treatment with DXR (Livingston *et al*., 1984; Carr *et al*., 1997). Such imbalances have been revealed also by *in vivo* studies (Fronczak *et al*., 1989; Noda *et al*., 1998), and it is considered that these circulatory imbalances are also caused by cardiac dysfunction induced by DXR. However, it is possible that DXR affects the vascular wall. During the course of i.v. injection of DXR, the vasculature is exposed to high levels of DXR, and *in vitro* studies have suggested that DXR acutely induces vascular smooth muscle to release Ca^{2+} from its intracellular storage site and causes direct vasoconstrictor (Kanmura *et al*., 1989) and vasodilator effects (Ferrans *et al*., 1997). Prior to the present study, however, no systematic investigations of mechanisms of vascular toxicity following repetitive and/or long-term therapy with DXR had been conducted.

In the present experiments, we examined the long-term effects of DXR on the morphology and functions of vascular smooth muscle using organ-cultured vascular tissue. An organ culture study has the following advantages: (1) it is

*Author for correspondence; E-mail: aozaki@mail.ecc.u-tokyo.ac.jp

possible to incubate tissues with a constant concentration of a drug for a long period of time; and (2) it is possible to observe changes in cell-to-cell interactions and in the extracellular matrix that are related to drug accumulation (Sethi *et al*., 1999).

Methods

Tissue preparation and organ culture procedure

Male Japanese White rabbits (2–3 kg) were euthanized by stunning and exsanguination. The organ culture procedure was performed as described previously (Yamawaki *et al*., 1999; 2000). Each artery was cut into rings approximately 2 mm wide, and the endothelium was removed by gently rubbing the intimal surface with forceps. The removal of endothelium was confirmed by the absence of relaxation caused by substance P (0.1 μM). Arterial rings were then placed in 2 ml Dulbecco's Modified Eagle Medium (DMEM) supplemented with 1% penicillin-streptomycin. The muscle rings were maintained at 37°C in an atmosphere of 95% air and 5% CO_2. Animal care and treatment conformed with the institutional guidelines of The University of Tokyo.

Measurement of muscle tension

Muscle tension was measured as described previously (Yamawaki *et al*., 1999; 2000). After the incubation, each arterial ring was attached to a holder under a resting tension of 10 mN. In another series of experiments, the arterial rings were cut into small rings (0.3 mm wide) and permeabilized with *Staphylococcal* α-toxin according to the method described previously (Nishimura *et al*., 1988). Each arterial ring was attached to a holder under a resting tension of 1 mN. In sets of both experiments, muscle tension was recorded isometrically with a force displacement transducer (Orientic, Japan). The amplitude of contractions was expressed as mN mg^{-1} wet weight or mN mm^{-2} tissue area.

Western blot analysis

Equal amounts (50 μg) of protein from the arterial rings were loaded onto 7.5% SDS-polyacrylamide gel electrophoresis and transferred to polyvinylidene difluoride (PVDF) membrane. The first antibodies were goat anti-α_{1A}-adrenoceptor polyclonal antibodies and rabbit anti-ET_A-receptor polyclonal antibodies, respectively (1 : 500 dilution). After the secondary antibody reaction, the membranes were treated with 0.05% 3,3′-diaminobenzine tetrahydrochloride (DAB) solution containing 0.01% H_2O_2. The densitometric intensity was quantified by NIH Imaging. To ensure that the same amounts of proteins were loaded, we confirmed that the same densitometric intensities of actin were observed in each preparation. The results were expressed as the ratio of the densitometric intensity of control arteries.

Quantitative RT–PCR

The oligonucleotide primers for the α_{1A}-adrenoceptor and the ET_A-receptor were designed from the cDNA database. The forward primers and reverse primers were designed as follows: ATCATATACCCATGCTCCAG (α_{1A}-adrenoceptor forward primer), GGGGCATGGAAGAGAAAAAA (α_{1A}-adrenoceptor reverse primer), CTATTGCCCACAGCAGAC (ET_A-receptor forward primer), and GGGAGATCAATGACCAC (ET_A-receptor reverse primer). And the oligonucleotide primers for GAPDH were TCCCTCAAGATTGTCAGCAA (forward primer) and AGATCCACAACGGATACATT (reverse primer), as described previously (Nishida *et al*., 1992). PCR products in 27–39 cycles (3 cycle interval) were electrophoresed onto 2% agarose gel containing 0.1% ethidium bromide and were detected using a UV-transilluminator. The densitometric intensity at 30 cycles was quantified by NIH Imaging. The results were expressed as the ratio of the densitometric intensity of GAPDH of each artery.

Morphological examination

The 4-μm-thick sections were stained with hematoxylin and eosin (HE). For the detection of apoptosis, sections were applied to the terminal deoxynucleotidyl transferase-mediated dUTP nick-end labelling (TUNEL) method was applied to the sections using the In Situ Apoptosis Detection Kit-POD (Boehringer Mannheim, Japan). For visualization, the sections were treated with 0.05% DAB solution containing 0.01% H_2O_2 with haematoxylin counterstaining. TUNEL-positive apoptotic nuclei were identified by the presence of dark brown staining. The densitometric intensity of these nuclei were quantified by NIH Imaging and the TUNEL-positive nuclei were counted. The results were expressed as a percentage of the total number of nuclei in the medial layer.

Analysis of DNA fragmentation

Four micrograms of each extracted DNA was electrophoresed onto a 2.0% agarose gel containing 0.1 % ethidium bromide and detected using an UV-transilluminator.

Statistical analysis

The results of the experiments are expressed as means ± s.e.mean. Statistical evaluation of the data was performed by unpaired Student's *t*-test for comparisons between two groups, and by one-way analysis of variance (ANOVA) followed by Dunnett's test for comparisons between more than two groups. A value of $P<0.05$ was taken as significant.

Drugs

The chemicals used were as followed; doxorubicin, superoxide dismutase (Sigma, U.S.A.), ethidium bromide solution, penicillin-streptomycin (GIBCO BRL, U.S.A.), DAB (Dojindo Laboratories, Japan), noradrenaline (Wako Pure Chemical, Japan), DMEM (Nissui Pharmaceutical, Japan), endothelin-1 (Peptide institute, Japan), goat anti-α_{1A}-adrenoceptor polyclonal antibody (Santa Cruz Biotechnology, U.S.A.), *Staphylococcal* α-toxin (donated by Dr I. Kato, Chiba University, Japan), anti-ET_A-receptor rabbit polyclonal antibody (donated by Dr T. Okada, Novartis Co., Japan), calyculin-A (donated by Dr N. Fusetani, The University of Tokyo, Japan).

Results

Muscle contractility in cultured tissue

Figure 1 shows the time-dependent changes in the contractions induced by noradrenaline (NA) and endothelin-1 (ET-1) in the tissue cultured in DMEM. NA- and ET-1-induced contractions decreased gradually with time. In the presence of 1 μM DXR, on the other hand, contractions elicited by 10 μM NA or 100 nM ET-1 were inhibited in a time-dependent manner, and contractions were almost completely suppressed after 5 days of incubation.

Figure 2 shows the effect of different concentrations of DXR on the concentration-response curves for NA, ET-1, and high K^+. In the arteries cultured without DXR for 7 days (control arteries), the cumulative addition of NA induced contractions in a concentration-dependent manner with an EC_{50} value of 6.6 ± 1.3 μM and a maximum force of 36.0 ± 4.2 mN mg^{-1} wet weight ($n = 17$) (Figure 2A). The NA-induced contractions were strongly inhibited in the arteries that had been treated with 0.3 μM DXR for 7 days ($n = 5$). In the arteries treated with 1 and 10 μM DXR for 7 days, the NA-induced contractions were completely abolished ($n = 12$ and 6, respectively).

In the control arteries, the cumulative addition of ET-1 induced concentration-dependent contractions with an EC_{50} value of 26.8 ± 12.6 nM and a maximum force of 32.8 ± 4.5 mN mg^{-1} wet weight ($n = 14$) (Figure 2B). Treating the arteries with 0.3 μM DXR for 7 days did not change the ET-1-induced contractions (the maximum force was 29.3 ± 2.8 mN mg^{-1} wet weight, $n = 5$). However, the ET-1-induced contractions were strongly in-

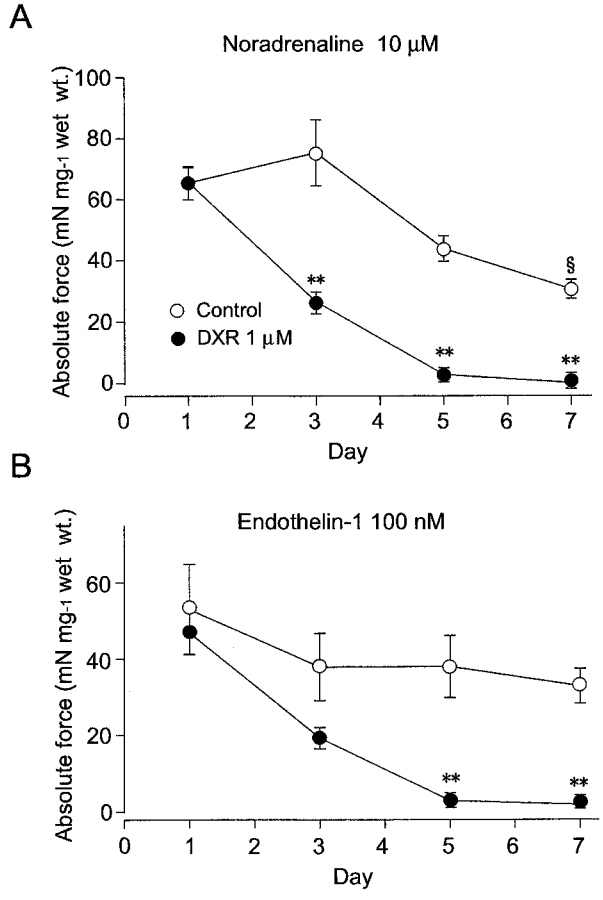

Figure 1 Time-dependent changes in contractions induced by noradrenaline (A) and endothelin-1 (B) after cultivation in DMEM with or without 1 μM DXR. Noradrenaline (10 μM) or endothelin-1 (100 nM) was added to rabbit mesenteric arteries cultured in DMEM for 1, 3, 5, and 7 days in the absence (control) or presence of 1 μM DXR. Results are expressed as means$\pm$s.e.mean ($n = 5-15$). **Significantly different from the results in control arteries at $P < 0.01$. §Significantly different from the results in control arteries after cultivation for 1 day at $P < 0.01$.

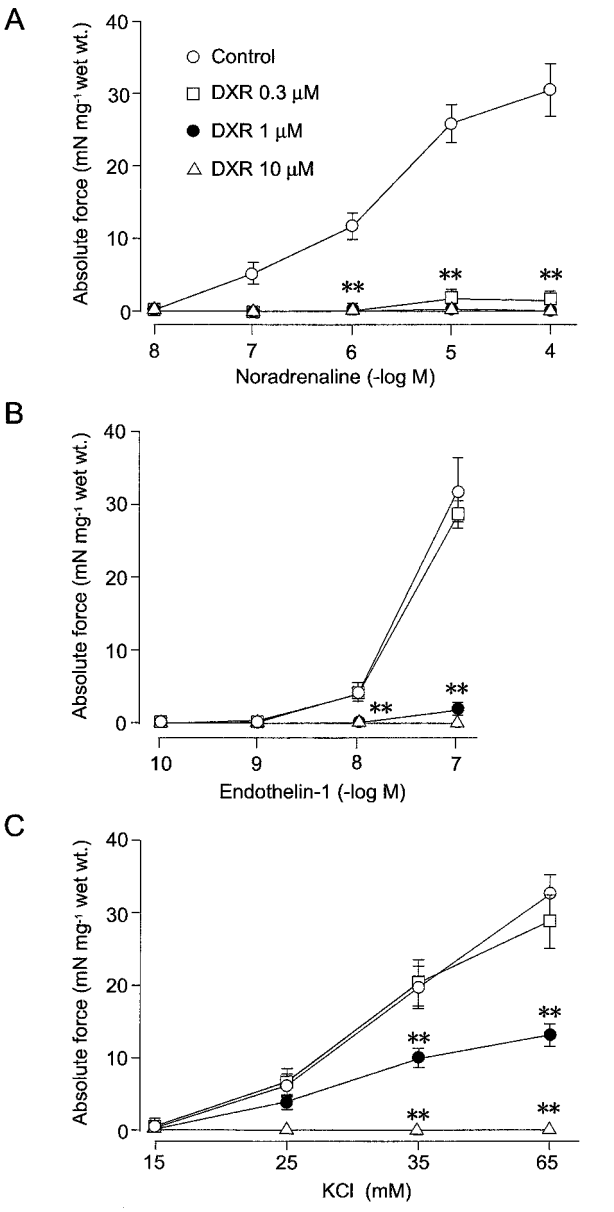

Figure 2 Chronic effect of various concentrations of DXR on contractions induced by noradrenaline (A), endothelin-1 (B), and high K^+ (C). Noradrenaline (0.01–100 μM), endothelin-1 (0.1–100 nM), or high K^+ (15.4–65.4 mM) was added cumulatively. Results are expressed as means$\pm$s.e.mean ($n = 5-15$). **Significantly different from results in control arteries at $P < 0.01$.

hibited in the arteries treated with 1 or 10 μM DXR ($n=21$, each).

In the control arteries, high K^+ induced contractions with a maximum force of 32.5 ± 2.7 mN mg^{-1} wet weight ($n=13$) (Figure 2C). Treatment with 0.3 μM DXR did not change the high K^+-induced contractions (the maximum force was 28.9 ± 3.8 mN mg^{-1} wet weight, $n=8$). In the 1 or 10 μM DXR-treated arteries, in contrast, the contractions induced by high levels of K^+ were inhibited in a concentration-dependent manner ($n=10$ and 5, respectively)

Western blot analysis for the α_{1A}-adrenoceptor and the ET_A-receptor

As shown in Figure 3A, the protein preparations extracted from the control arteries showed a typical band with a molecular mass of about 68 kDa, a value that is in agreement with earlier results (Hu *et al*., 1996). In the protein preparations extracted from 0.3 μM DXR-treated arteries for 7 days, the expression of α_{1A}-adrenoceptor protein was decreased to 0.22 ± 0.02 of the control ($n=5$). On the other hand, the ET_A-receptor expression (with a molecular mass of about 72 kDa) was not changed in the 0.3 μM DXR-treated arteries (0.98 ± 0.04 of control) ($n=4$).

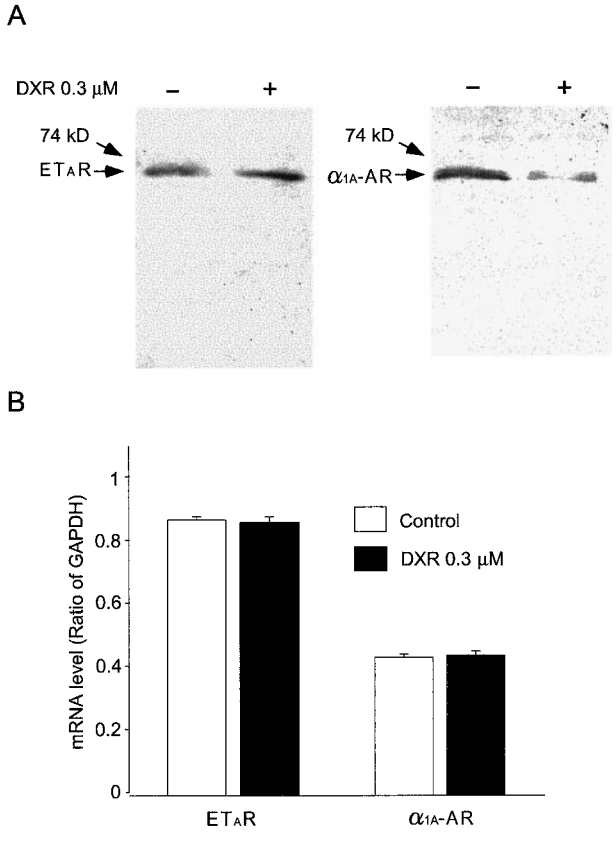

Figure 3 Chronic effect of 0.3 μM DXR on α_{1A}-adrenoceptor (α_{1A}-AR) protein and mRNA expression. (A) Shows a typical trace of the 4–5 experiments in Western blot analysis for ET_A-receptor (ET_A-R) and α_{1A}-adrenoceptor (α_{1A}-AR) protein expression. (B) Shows quantitative RT–PCR for the determination of mRNA of the ET_A-receptor (ET_A-R) and the α_{1A}-adrenoceptor (α_{1A}-AR). The results were expressed as the ratio of GAPDH of each artery at 30 cycles.

Expression of α_{1A}-adrenoceptor mRNA

We examined the effects of DXR on the mRNA level of the α_{1A}-adrenoceptor and the ET_A-receptor using quantitative RT–PCR. The amplification at 27–39 cycles showed a similar increase in RNA signals for the α_{1A}-adrenoceptor (244 basepairs), the ET_A-receptor (204 basepairs), and GAPDH (308 basepairs) in the control and the 0.3 μM DXR-treated arteries (7 days) (data not shown). As shown in Figure 3B, the expression of RT–PCR products encoding the α_{1A}-adrenoceptor and the ET_A-receptor did not differ between the control arteries and the 0.3 μM DXR-treated arteries at 30 cycles of amplification (ratio ET_A-receptor/GAPDH: control, 0.86 ± 0.01; 0.3 μM DXR, 0.85 ± 0.02; ratio α_{1A}-adrenoceptor/GAPDH: control, 0.42 ± 0.01; 0.3 μM DXR, 0.43 ± 0.03) ($n=4$, each).

Effect of superoxide dismutase (SOD) on DXR-induced impairment of NA-induced contractions

To further clarify the mechanism of the inhibitory effect of DXR on NA-induced contractions, we examined the effect of SOD, a suppressor of free radicals to hydrogen peroxide. Arteries were cultured in the presence of 0.3 μM DXR with or without 50, 100, and 200 u ml^{-1} SOD for 7 days. Muscles treated with SOD (50 or 100 u ml^{-1}) markedly recovered from the NA-induced contractions in a concentration-dependent manner (from 1.46 ± 0.28 mN mg^{-1} wet weight to 6.97 ± 0.7 or to 8.04 ± 0.48 mN mg^{-1} wet weight, respectively) ($n=7$, each) (Figure 4A). On the other hand, in the arteries treated with 0.3 μM DXR and 200 u ml^{-1} SOD for 7 days, this recovery was not obvious (1.01 ± 0.73 mN mg^{-1} wet weight). In addition, we examined the effects of 100 u ml^{-1} SOD on α_{1A}-adrenoceptor expression (Figure 4B), and found that α_{1A}-adrenoceptor protein expression in the 0.3 μM DXR-treated arteries also recovered from 0.22 ± 0.02 ($n=5$) to 0.82 ± 0.04 ($n=5$) after the SOD treatment (Figure 4B).

Muscle contractility in the α-toxin permeabilized muscle

Figure 5A shows the effect of DXR on myogenic muscle contractility in the permeabilized muscle. To obtain the maximum contractile force, a myosin light chain was maximally phosphorylated by 1 μM calyculin-A, a potent inhibitor of myosin phosphatase (Ishihara *et al*., 1989), at pCa^{2+} 4.5. In the control arteries, the maximum force was 0.54 ± 0.07 mN mm^{-2} ($n=8$). Although the maximal force did not change in the 0.3 μM DXR-treated arteries (7 days) (0.51 ± 0.07 mN mm^{-2}, $n=8$), the contractile activity was significantly decreased in the 1 μM DXR-treated arteries (0.19 ± 0.06 mN mm^{-2}; $n=8$, $P<0.01$). The contractile activity was almost abolished in the arteries cultured with 10 μM DXR ($n=8$).

Figure 5B shows the effects of DXR on the pCa^{2+}-force relationship. Treatment of the muscle with 0.3 and 1 μM DXR for 7 days had no effect on the relationship with EC_{50} values (control, 6.1 ± 0.1; 0.3 μM DXR, 5.9 ± 0.1; 1 μM DXR, 5.9 ± 0.1).

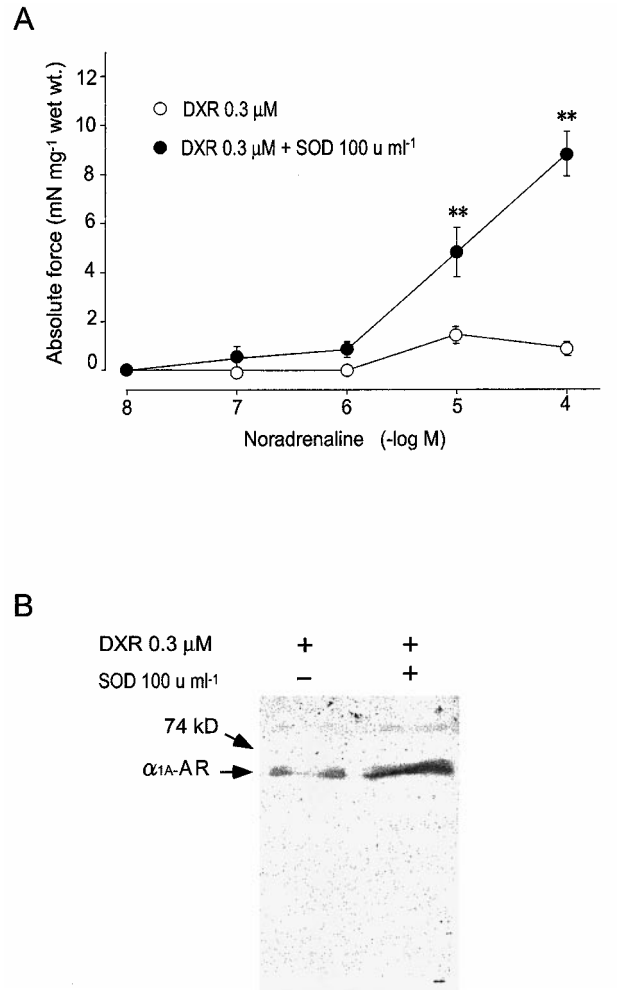

Figure 4 The effects of SOD (100 u ml^{-1}) on DXR (0.3 μM)-induced inhibition of noradrenaline-induced contractions (A) and α_{1A}-adrenoceptor (α_{1A}-AR) protein expression (B). Results are expressed as means $\pm$ s.e.mean ($n=5-7$). (B) Shows a typical result of the five experiments in Western blot analysis for α_{1A}-adrenoceptor (α_{1A}-AR) protein expression. **Significantly different from results in DXR treated arteries at $P<0.01$.

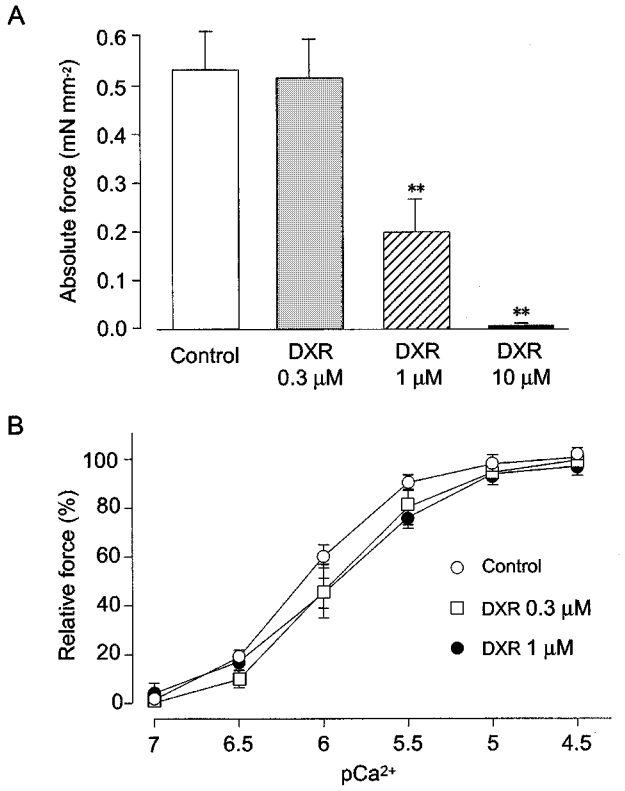

Figure 5 Chronic effect of DXR on muscle contractility in the permeabilized rabbit mesenteric artery. (A) Shows the maximum contractile capability induced by adding 30 μM Ca^{2+} with 1 μM calyculin-A. (B) Shows the pCa^{2+}-tension relationship. 100% represents the maximum force induced by 30 μM Ca^{2+} with 1 μM calyculin-A. **Significantly different from results in control arteries at $P<0.01$.

Morphological examination

Figure 6 shows the effect of DXR on the morphology of the artery. In the medial layer of the control arteries, the flat-shaped smooth muscle cells were arranged in an ordinary manner (Figure 6A). In the medial layer of the arteries treated with 0.3 μM DXR for 7 days, several smooth muscle cells appear shrivelled, and occasional apoptosis-like cells were observed (Figure 6B). In the medial layer of the 1 μM DXR-treated arteries, typical apoptotic cells, in which nuclei were concentrated, rounded, and surrounded by a rim of red reaction product, were observed (Figure 6C). The orientation of the smooth muscle cells was generally lost in these arteries. In the medial layer of the 10 μM DXR-treated arteries, the orientation of the smooth muscle cells was also lost, nuclear swelling and karyolysis were observed, and the intensity of the cytoplasm staining was decreased, indicating that necrotic changes had taken place (Figure 6D).

Figure 7 shows the TUNEL-staining sections. In the medial layer of the control, the 0.3 μM DXR-, and the 10 μM DXR-treated arteries (7 days), TUNEL-positive staining was almost invisible (control, $1.5\pm0.2\%$; 0.3 μM DXR, $4.5\pm0.6\%$; 10 μM DXR, $1.6\pm0.2\%$; $n=6$, each) (Figure 7Aa,b,d). In the medial layer of these arteries, however, weak brown staining for TUNEL was observed. This weak staining was probably due to the nicks in DNA caused by the cutting of sections or to physiological nicks or necrotic changes. In the medial layer of the 1 μM DXR-treated arteries, in contrast, TUNEL-positive, dark brown nuclei were often observed ($42.6\pm2.0\%$, $n=5$) (Figure 7Ac, arrow heads). In the arteries treated with 1 μM DXR for 5 days, few TUNEL-positive cells were detected (data not shown).

Analysis of DNA fragmentation

We further examined the internucleosomal DNA fragmentation using gel electrophoresis (Figure 7B). In the control and the 0.3 μM DXR-treated arteries (7 days), no DNA cleavage was visualized. In the 1 μM DXR-treated arteries, in contrast, DNA cleavage bands with a pattern characteristic of an internucleosomal ladder were observed. Such DNA fragmentation was not obvious in the arteries treated with 1 μM DXR for 5 days (data not shown). Additionally, in the preparation isolated from the 10 μM DXR-treated arteries, random

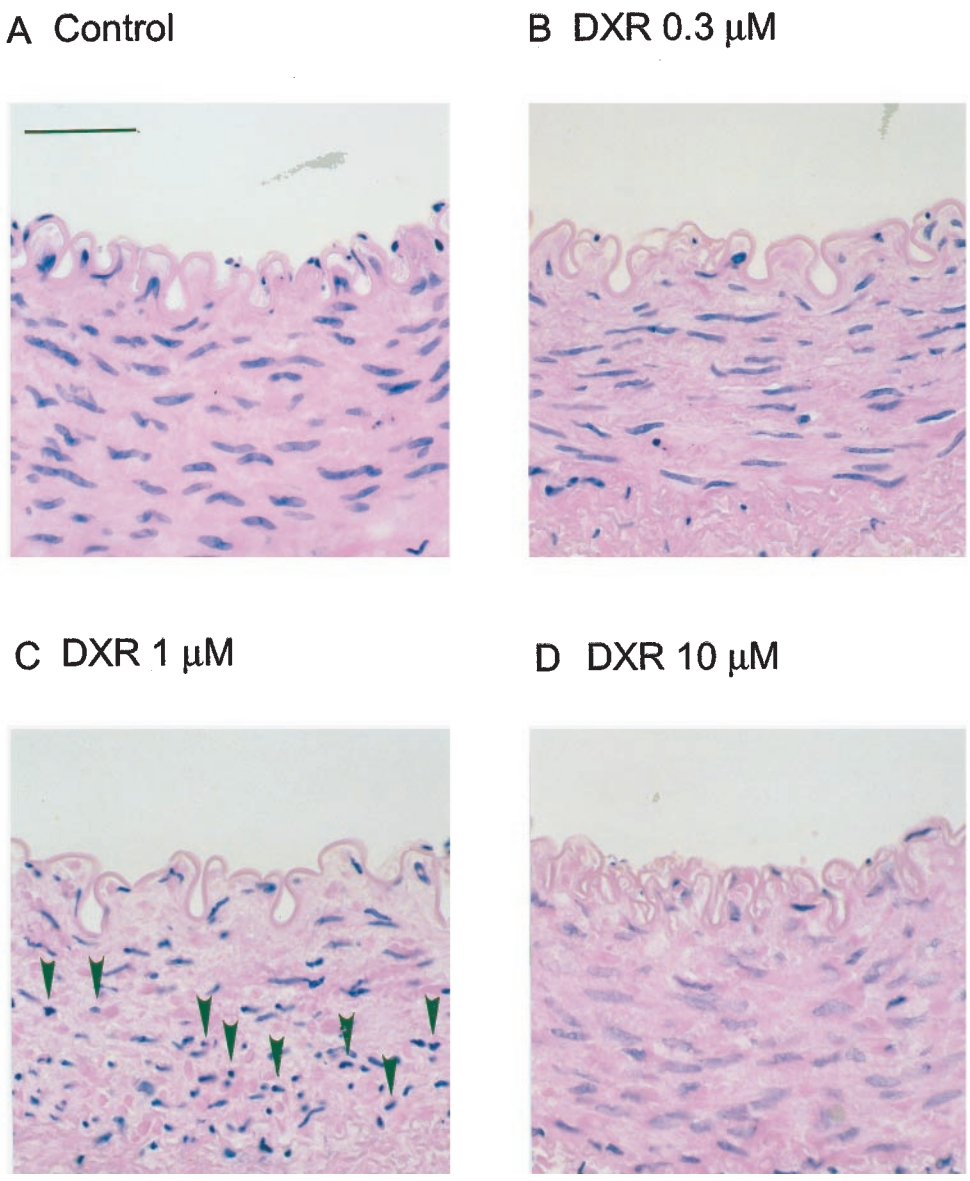

Figure 6 Representative light micrographs of sections stained with hematoxylin and eosin in rabbit mesenteric arteries chronically treated with DXR for 7 days. Arrow heads indicate typical apoptotic smooth muscle cells. Magnification: × 184. Bar, 85 μm.

fragmentation of DNA (smearing of DNA) associated with necrosis was observed.

Discussion

In the preliminary experiments, we examined the acute effect of DXR on smooth muscle contractility in a freshly isolated artery and found that DXR induced neither contraction nor relaxation at a dosage of 0.3–10 μM. We also examined the effects of serum-free organ culture on smooth muscle morphology and contractility (Figures 1, 2, 4 and 6), and confirmed that smooth muscle morphology was well maintained and smooth muscle contractility was preserved in the rabbit mesenteric arteries cultured in the serum-free DMEM for 7 days, as reported previously (Webb & Karaki 1999; Yamawaki *et al*., 2000).

In the present experiments, we examined the effects of DXR on arterial contractility and found that treatment with 0.3 μM DXR for 7 days selectively inhibited the NA-induced contractions (Figure 2A). However, the absolute force and Ca^{2+}-sensitivity of the permeabilized muscles did not change, and no remarkable morphological changes were observed in the 0.3 μM DXR-treated arteries (Figure 6). To elucidate the mechanisms of the impairment of vascular contraction, we examined the expression of the α_{1A}-adrenoceptor and ET_A-receptor proteins (Figure 3A). We found that the culture with 0.3 μM DXR decreased the expression of the α_{1A}-adrenoceptor but not that of the ET_A-receptor, suggesting that down-regulation of the α_{1A}-adrenoceptor protein plays a critical role in decreases in the NA-induced contractions. Additionally, we found that α_{1A}-adrenoceptor mRNA expression in the 0.3 μM DXR-treated arteries did not differ from that in the control arteries (Figure 3B). Cardiotoxicity

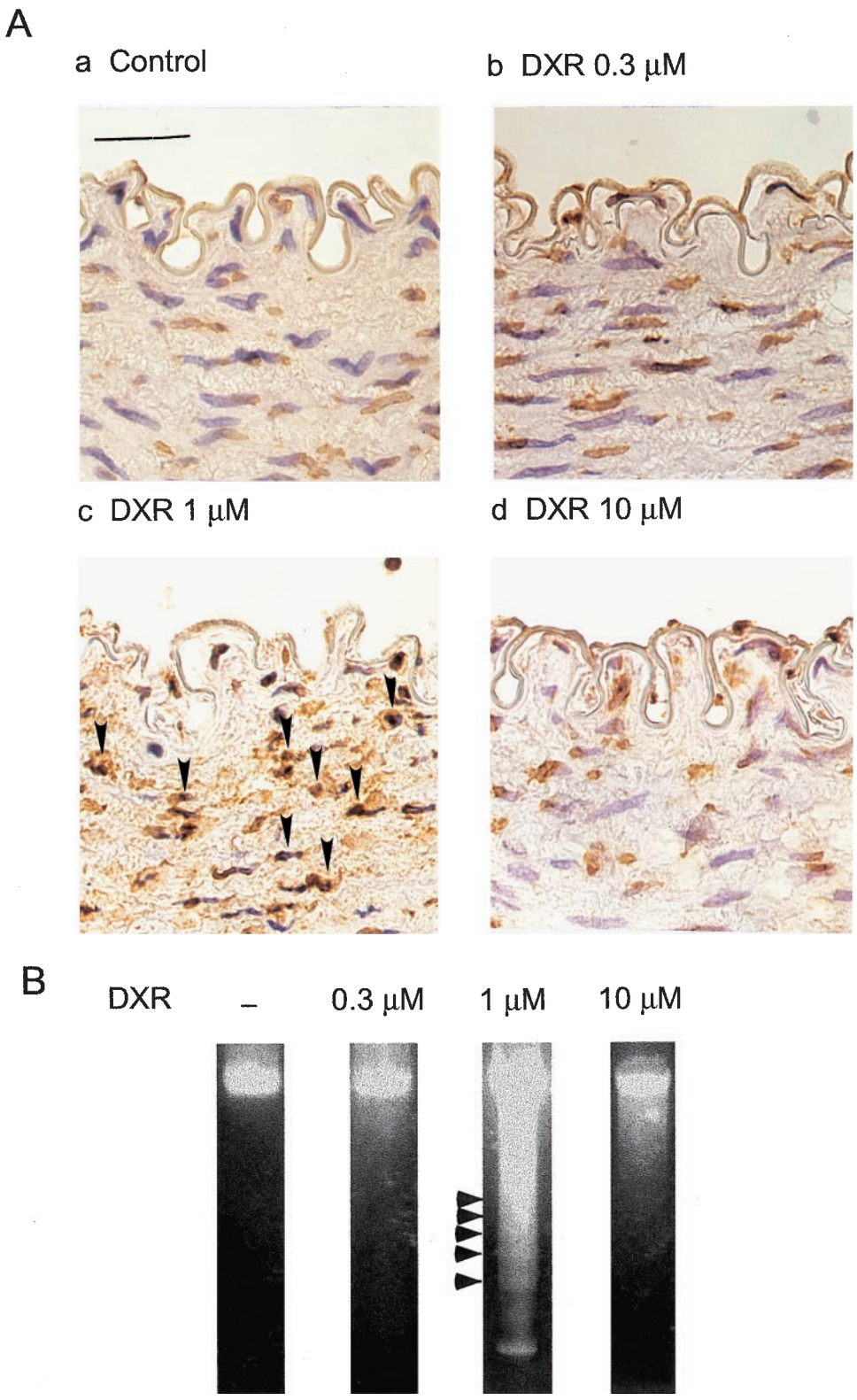

Figure 7 Detection of apoptosis induced by chronic treatment with DXR for 7 days. (A) Shows the results of TUNEL assay. Arrow heads indicate TUNEL-positive smooth muscle cells. Magnification: × 304. Bar, 50 μm. (B) Shows the results of the DNA ladder formation assay using gel electrophoresis.

of DXR is considered to be mediated by the production of superoxide radical anions produced by oxidation/reduction cycling of DXR (Jeyaseelan *et al*., 1997). In the present study, SOD, which induces the formation of hydrogen peroxide from superoxide anion radicals, significantly restored the NA-induced contraction in the 0.3 μM DXR-treated arteries along

with α_{1A}-adrenoceptor protein expression (Figure 4). These results indicate that superoxide radical anions produced by oxidation-reduction cycling may be related to the down-regulation of the α_{1A}-adrenoceptor at the protein synthesis step. However, after SOD-treatment, vascular muscle contractility (Figure 4A) did not recover at a rate proportional to the recovery ratio of α_{1A}-adrenoceptor expression (contractility, 15.3% recovery; protein expression, 60% recovery) (Figure 4B). It has been reported that free radicals alter the higher order structure of protein, and result in a depletion of its functional characteristics (Wratten *et al*., 2000). Therefore, one possible explanation for this discrepancy is that, although protein expression was recovered, its function was not recovered fully. Further study is needed to examine this possibility. Dalske & Hardy (1988) examined the contractility of aortic smooth muscle isolated from rat to which a low dose of DXR had been administered for 4 weeks, and found that the low-dose treatment with DXR attenuated the NA-induced contractions of the aorta *in vivo* without any signs of toxicity in cardiac muscle. Taken together, these results suggest that the sympathetic regulation of vascular contraction is impaired by low doses of DXR through reduction in the α_{1A}-adrenoceptor. Mechanism for selective down-regulation of the α_{1A}-adrenoceptor protein was not clarified in the present experiments.

Treatment of the arteries with a higher concentration (1 μM) of DXR for 7 days nonselectively inhibited the contractilities of intact and permeabilized muscles (Figures 2 and 5A). Furthermore, in the 1 μM DXR-treated arteries, morphological examinations revealed the existence of concentrated nuclei (Figure 6) and TUNEL-positive smooth muscle cells (Figure 7A). Formation of internucleosomal DNA fragmentation was also visualized (Figure 7B). The DNA fragmentation in the 1 μM DXR-treated vascular tissue was not visualized so clearly as compared with that in the results obtained in cultured cells. This may be due to the low ratio of the apoptotic cells as shown in TUNEL assay ($42.6 \pm 2.0\%$). These results suggest that chronic treatment of rabbit mesenteric arteries with 1 μM DXR induces apoptosis in smooth muscle cells. This may be at least partly responsible for the decreased smooth muscle contractility.

In various cell lines, it has been reported that DXR, within several hours of administration, induces apoptosis that is mediated by Fas-dependent or Fas-independent pathways (Gamen *et al*., 1997; Fulda *et al*., 1997). On the other hand, recent studies have documented the occurrence of a delayed type of apoptosis *in vivo* and *vitro* (Zhang *et al*., 1996; Zaleskis *et al*., 1994; Delpy *et al*., 1999) that can take place after treatment with DXR for several days. In the present study, the arteries treated with 1 μM DXR for 5 days showed few apoptosis-positive cells in a TUNEL assay and no DNA fragmentation (data not shown). Therefore, it is possible that the apoptosis observed in the arteries treated with 1 μM DXR for 7 days is the delayed type.

Treatment with 10 μM DXR for 7 days completely suppressed the contractility of intact and permeabilized muscles (Figures 2 and 5A). Morphological examinations revealed the existence of swelling nuclei and karyolysis in smooth muscle cells (Figure 6). Additionally, random fragmentation of DNA was observed in gel electrophoresis (Figure 7B). These results suggest that 10 μM DXR elicited necrosis, which may explain the abolishment of smooth muscle contractility. It has been reported that necrotic changes are induced in various types of cells by treatment with high concentrations of DXR (Muller *et al*., 1997; Toyota *et al*., 1998). In these reports, the authors speculated that at high concentrations, DXR may stimulate the apoptotic program, although the program could not be completed because of the inhibition of protein synthesis at the level of transcription.

The plasma level of DXR has been estimated to reach 1 μM immediately after treatment, and the sustained plasma levels during chemotherapy are close to 0.2 μM (Young *et al*., 1981). Therefore, the concentrations of DXR (0.3 and 1 μM) used in the present study are considered to be within the range of plasma concentrations during DXR therapy.

In summary, the present results demonstrated for the first time that DXR induces apoptotic and necrotic morphological changes at therapeutic (1 μM) and toxic (10 μM) concentrations, respectively, in vascular smooth muscle. These changes may result in a decrease in vascular smooth muscle contractility. In addition, DXR at a lower concentration (0.3 μM) selectively inhibited α_{1A}-adrenoceptor expression. This inhibition might be induced by a mechanism independent of programmed cell death. These findings may be helpful for the management of cardiovascular toxicity during cancer chemotherapy.

This work was partly supported by a Grant-in-Aid for scientific research from the Ministry of Education, Japan. Anti-ET_A-receptor rabbit polyclonal antibody and *Staphylococcal* α-toxin was donated by Dr T. Okada (Novartis Co., Tokyo, Japan) and Dr I. Kato (Chiba University, Japan), respectively.

References

CARR, B.I., ZAJKO, A., BRON, K., ORONS, P., SAMMON, J. & BARON, R. (1997). Phase II study of Spherex (degradable starch microspheres) injected into the hepatic artery in conjunction with doxorubicin and cisplatin in the treatment of advanced-stage hepatocellular carcinoma: interim analysis. *Semin. Oncol.,* **24,** S6-97 – S6-99.

CHUANG, R.Y. & CHUANG, L.F. (1979). Inhibition of chicken myeloblastosis RNA polymerase II activity by adriamycin. *Biochemistry,* **18,** 2069 – 2073.

DALSKE, H.F. & HARDY, K. (1988). Effect of low-dose doxorubicin on calcium content and noradrenaline response in rat aorta. *Eur. J. Cancer Clin. Oncol.,* **24,** 979 – 983.

DELPY, E., HATEM, S.N., ANDRIEU, N., DE-VAUMAS, C., HENAFF, M., RUCKER-MARTIN, C., JAFFREZOU, J.P., LAURENT, G., LEVADE, T. & MERCADIER, J.J. (1999). Doxorubicin induces slow ceramide accumulation and late apoptosis in cultured adult rat ventricular myocytes. *Cardiovasc. Res.,* **43,** 398 – 407.

FERRANS, V.J., CLARK, J.R., ZHANG, J., YU, Z.X. & HERMAN, E.H. (1997). Pathogenesis and prevention of doxorubicin cardiomyopathy. *Tsitologiia,* **39,** 928 – 937.

FRONCZAK, A., DRZEWOSKI, J. & POLAKOWSKI, P. (1989). Comparative studies of doxorubicin and 4′-epidoxorubicin effects on cardiovascular system in rabbits. *Pol. J. Pharmacol. Pharm.,* **41,** 597 – 609.

FULDA, S., SIEVERTS, H., FRIESEN, C., HERR, I. & DEBATIN, K.M. (1997). The CD95 (APO-1/Fas) system mediates drug-induced apoptosis in neuroblastoma cells. *Cancer Res.,* **57,** 3823 – 3829.

GAMEN, S., ANEL, A., LASIERRA, P., ALAVA, M.A., MARTINEZ-LORENZO, M.J., PINEIRO, A. & NAVAL, J. (1997). Doxorubicin-induced apoptosis in human T-cell leukemia is mediated by caspase-3 activation in a Fas-independent way. *FEBS Lett.,* **417,** 360 – 364.

HU, Z.W., SHI, X.Y. & HOFFMAN, B.B. (1996). Insulin and insulin-like growth factor I differentially induce alpha1-adrenoceptor subtype expression in rat vascular smooth muscle cells. *J. Clin. Invest.,* **98,** 1826 – 1834.

ISHIHARA, H., MARTIN, B.L., BRAUTIGAN, D.L., KARAKI, H., OZAKI, H., KATO, Y., FUSETANI, N., WATABE, S., HASHIMOTO, K. & UEMURA, D. (1989). Calyculin A and okadaic acid: inhibitors of protein phosphatase activity. *Biochem. Biophys. Res. Commun.,* **159,** 871 – 877.

JEYASEELAN, R., POIZAT, C., WU, H.Y. & KEDES, L. (1997). Molecular mechanisms of doxorubicin-induced cardiomyopathy. Selective suppression of Reiske iron-sulfur protein, ADP/ATP translocase, and phosphofructokinase genes is associated with ATP depletion in rat cardiomyocytes. *J. Biol. Chem.,* **272,** 5828 – 5832.

KANMURA, Y., RAEYMAEKERS, L. & CASTEELS, R. (1989). Effects of doxorubicin and ruthenium red on intracellular Ca^{2+} stores in skinned rabbit mesenteric smooth-muscle fibres. *Cell. Calcium,* **10,** 433 – 439.

KUSUMOTO, H., RODGERS, Q.E., BOEGE, F., RAIMONDI, S.C. & BECK, W.T. (1996). Characterization of novel human leukemic cell lines selected for resistance to merbarone, a catalytic inhibitor of DNA topoisomerase II. *Cancer Res.,* **56,** 2573 – 2583.

LIVINGSTON, R.B., STEPHENS, R.L., BONNET, J.D., GROZEA, P.N. & LEHANE, D.E. (1984). Long-term survival and toxicity in small cell lung cancer. Southwest Oncology Group study. *Am. J. Med.,* **77,** 415 – 417.

MULLER, I., JENNER, A., BRUCHELT, G., NIETHAMMER, D. & HALLIWELL, B. (1997). Effect of concentration on the cytotoxic mechanism of doxorubicin-apoptosis and oxidative DNA damage. *Biochem. Biophys. Res. Commun.,* **230,** 254 – 257.

NISHIDA, K., HARRISON, D.G., NAVAS, J.P., FISHER, A.A., DCKERY, S.P., UEMATSU, M., NEREM, R.M., ALEXANDER, R.W. & MURPHY, T.J. (1992). Molecular cloning and characterization of the constitutive bovine aortic endothelial cell nitric oxide synthase. *J. Clin. Invest.,* **90,** 2092 – 2096.

NISHIMURA, J., KOLBER, M. & VAN BREEMEN, C. (1988). Noradrenaline and GTP γS increase myofilament Ca^{2+} sensitivity in α-toxin permeabilized arterial smooth muscle. *Biochem. Biophys. Res. Commun.,* **157,** 677 – 683.

NODA, T., WATANABE, T., KOHDA, A., HOSOKAWA, S. & SUZUKI, T. (1998). Chronic effects of a novel synthetic anthracycline derivative (SM-5887) on normal heart and doxorubicin-induced cardiomyopathy in beagle dogs. *Invest. New Drugs,* **16,** 121 – 128.

SETHI, T., RINTOUL, R.C., MOORE, S.M., MACKINNON, A.C., SALTER, D., CHOO, C., CHILVERS, E.R., DRANSFIELD, I., DONNELLY, S.C., STRIETER, R. & HASLETT, C. (1999). Extracellular matrix proteins protect small cell lung cancer cells against apoptosis: a mechanism for small cell lung cancer growth and drug resistance in vivo. *Nat. Med.,* **5,** 662 – 668.

TOYOTA, N., STREBEL, F.R., STEPHENS, L.C., MATSUDA, H., OSHIRO, T., JENKINS, G.N. & BULL, J.M. (1998). Therapeutic efficacy and apoptosis and necrosis kinetics of doxorubicin compared with cisplatin, combined with whole-body hyperthermia in a rat mammary adenocarcinoma. *Int. J. Cancer,* **76,** 499 – 505.

VON, HOFF, D.D., LAYARD, M.W., BASA, P., DAVIS, JR. H.L., VON, HOFF, A.L., ROZENCWEIG, M. & MUGGIA, F.M. (1979). Risk factors for doxorubicin-induced congestive heart failure. *Ann. Intern. Med.,* **91,** 710 – 717.

WEBB, R.C. & KARAKI, H. (1999). 4th US/Japan symposium on molecular and cellular aspects of vascular smooth muscle functions. Honolulu, Hawaii, USA, May 12 – 15, 1999. *J. Vasc. Res.,* **36,** 419 – 428.

WEISS, R.B., SAROSY, G., CLAGETT-CARR, K., RUSSO, M. & LEYLAND-JONES, B. (1986). Anthracycline analogs: the past, present, and future. *Cancer Chemother. Pharmacol.,* **18,** 185 – 197.

WRATTEN, M.L., TETTA, C., URSINI, F. & SEVANIAN, A. (2000). Oxidant stress in hemodialysis: prevention and treatment strategies. *Kidney Int.,* **58,** 76, S126 – S132.

YAMAWAKI, H., SATO, K., HORI, M., OZAKI, H., NAKAMURA, S., NAKAYAMA, H., DOI, K. & KARAKI, H. (1999). Impairment of EDR by a long-term PDGF treatment in organ-cultured rabbit mesenteric artery. *Am. J. Physiol.,* **277,** H318 – H323.

YAMAWAKI, H., SATO, K., HORI, M., OZAKI, H., NAKAMURA, S., NAKAYAMA, H., DOI, K. & KARAKI, H. (2000). Morphological and functional changes of rabbit mesenteric artery cultured with fetal bovine serum. *Life Sci.,* **67,** 807 – 820.

YOUNG, R.C., OZOLS, R.F. & MYERS, C.E. (1981). The anthracycline antineoplastic drugs. *N. Engl. J. Med.,* **305,** 139 – 153.

ZALESKIS, G., HO, R.L., DIEGELMAN, P., MACCUBBIN, D., UJHAZY, P., MIHICH, E. & EHRKE, M.J. (1994). Intracellular doxorubicin kinetics in lymphoma cells and lymphocytes infiltrating the tumor area in vivo: a flow cytometric study. *Oncol. Res.,* **6,** 183 – 194.

ZHANG, J., CLARK, J.R., HERMAN, E.H. & FERRANS, V.J. (1996). Doxorubicin-induced apoptosis in spontaneously hypertensive rats: differential effects in heart, kidney and intestine, and inhibition by ICRF-187. *J. Mol. Cell. Cardiol.,* **28,** 1931 – 1943.

(Received August 2, 2000
Revised January 4, 2001
Accepted January 19, 2001)